# An empirical model for prediction of geomagnetic storms using initially observed CME parameters at the Sun

R.-S. Kim,[1,2] K.-S. Cho,[3] Y.-J. Moon,[4] M. Dryer,[5] J. Lee,[6] Y. Yi,[1] K.-H. Kim,[4] H. Wang,[6] Y.-D. Park,[3] and Yong Ha Kim[1]

Received 2 February 2010; revised 28 July 2010; accepted 13 August 2010; published 14 December 2010.

[1] In this study, we discuss the general behaviors of geomagnetic storm strength associated with observed parameters of coronal mass ejection (CME) such as speed ($V$) and earthward direction ($D$) of CMEs as well as the longitude ($L$) and magnetic field orientation ($M$) of overlaying potential fields of the CME source region, and we develop an empirical model to predict geomagnetic storm occurrence with its strength (gauged by the *Dst* index) in terms of these CME parameters. For this we select 66 halo or partial halo CMEs associated with M-class and X-class solar flares, which have clearly identifiable source regions, from 1997 to 2003. After examining how each of these CME parameters correlates with the geoeffectiveness of the CMEs, we find several properties as follows: (1) Parameter $D$ best correlates with storm strength *Dst*; (2) the majority of geoeffective CMEs have been originated from solar longitude 15°W, and CMEs originated away from this longitude tend to produce weaker storms; (3) correlations between *Dst* and the CME parameters improve if CMEs are separated into two groups depending on whether their magnetic fields are oriented southward or northward in their source regions. Based on these observations, we present two empirical expressions for *Dst* in terms of $L$, $V$, and $D$ for two groups of CMEs, respectively. This is a new attempt to predict not only the occurrence of geomagnetic storms, but also the storm strength (*Dst*) solely based on the CME parameters.

**Citation:** Kim, R.-S., K.-S. Cho, Y.-J. Moon, M. Dryer, J. Lee, Y. Yi, K.-H. Kim, H. Wang, Y.-D. Park, and Y. H. Kim (2010), An empirical model for prediction of geomagnetic storms using initially observed CME parameters at the Sun, *J. Geophys. Res.*, *115*, A12108, doi:10.1029/2010JA015322.

## 1. Introduction

[2] Coronal mass ejections (CMEs) and their associated shock waves are important drivers of space weather as they can compress the magnetosphere and trigger geomagnetic storms [*Brueckner et al.*, 1998; *Gopalswamy et al.*, 2000]. The existing prediction schemes of geomagnetic storms rely on information close to the Earth, that is, solar wind speed and the southward component of the interplanetary magnetic field (IMF) which gives a very little time for warning [*Burton et al.*, 1975; *Tsurutani et al.*, 1998; *Tsurutani*, 2001 and references therein]. However, prediction schemes based on inputs involving CME properties close to the Sun will give us 2–3 days of forewarning. Only a few attempts have been made in this direction [*Srivastava*, 2005; *Song et al.*, 2006] and further refinement is desirable. We however note that it is yet to be determined whether information on CMEs can be sufficient for predicting the occurrence of the geomagnetic storms and perhaps their strengths. At least we know that only a subset of CMEs trigger geomagnetic storms.

[3] Several CME parameters have been proposed to describe the geoeffectiveness of CMEs. The frontside halo CMEs with large angular widths more than 120°, and which appear as expanding and circular brightening that surrounds the coronagraph occulting disk, are known to be geoeffective because they are directed toward the Earth [*Webb*, 2002; *Gopalswamy et al.*, 2007]. The CME source location and earthward speed are also important geoeffective parameters. Several studies suggested that fast halo CMEs, which occurred close to solar center, are favorable candidates for strong geomagnetic storms [*Venkatakrishnan and Ravindra*, 2003; *Kim et al.*, 2005]. *Wang et al.* [2002] found that 83% of the frontside halo CMEs that caused geomagnetic storms with $Kp \geq 5$ took place within ±30° of the central meridian and that their source locations are asymmetrical in longitude, with the majority located in the west side of the central

[1]Department of Astronomy and Space Science, Chungnam National University, Daejeon, Korea.
[2]NASA Goddard Space Flight Center, Greenbelt, Maryland, USA.
[3]Solar and Space Weather Research Group, Korea Astronomy and Space Science Institute, Daejeon, Korea.
[4]School of Space Research, Kyung Hee University, Yongin, Korea.
[5]National Oceanic and Atmospheric Administration, Boulder, Colorado, USA.
[6]Department of Physics, New Jersey Institute of Technology, Newark, New Jersey, USA.


0148-0227/10/2010JA015322

meridian. *Srivastava and Venkatakrishnan* [2004] showed that CME speeds in the Large Angle and Spectrometric Coronagraph (LASCO) field of view were roughly correlated with the strength of geomagnetic storms and that a large percentage (62%) of the geoeffective CMEs are faster than 700 km $s^{-1}$.

[4] The magnetic field orientation of a CME's source region is suggested to be an important parameter of geoeffective CME [*Pevtsov and Canfield*, 2001]. *Kang et al.* [2006] found that southward orientation of the magnetic field in the CME source region plays an important role in the production of geomagnetic storms by investigation of the source region's shapes (S or inverse-S) of the X-ray sigmoids associated with 63 CMEs. For about 84% of the CMEs, their geoeffective consequences are consistent with their magnetic field orientations. *Song et al.* [2006] investigated the relationship between magnetic structures of CME source regions and geomagnetic storms for 73 events. They defined the magnetic field orientation angle $\theta$ as the angle between the projection of the overlying potential field line on the solar surface and the direction toward the south pole. If $|\theta|$ is less than 90°, the magnetic field orientation of CME is southward, otherwise it is northward. They showed that 73% (22/30) of the CME source regions associated with intense geomagnetic storms ($Dst \leq -100$ nT) and 92% (12/13) of the CME source regions associated with super storms ($Dst \leq -200$ nT) have southward magnetic field orientations.

[5] Another important geoeffective parameter is the direction parameter, as defined by the ratio of the shortest to the longest distance of the CME front measured from the solar center [*Moon et al.*, 2005]. This parameter quantifies the degree of asymmetry of the CME shape and shows how much CME propagation is directed to Earth. *Kim et al.* [2008] examined the direction parameters and showed that CMEs with large direction parameter values ($D \geq 0.4$) are strongly associated with geomagnetic storms. According to their results, all CMEs associated with super storms ($Dst \leq -200$ nT) are found to have large direction parameters ($D \geq 0.6$) and the CMEs causing intense storms ($Dst \leq -100$ nT), in spite of their northward magnetic field, have large direction parameters ($D \geq 0.6$).

[6] The main concerns faced by the space weather prediction challenge are to predict the arrival time of a CME and its shock wave at the Earth and the occurrence and magnitude of a geomagnetic storm. Several empirical and physics-based models have been proposed to predict the CME or the CME-associated interplanetary (IP) shock arrival times based on their initial speeds [*Gopalswamy et al.*, 2001; *Dryer et al.*, 2004; *Kim et al.*, 2007]. As an empirical model for prediction of the geomagnetic storm occurrence, *Kim et al.* [2005, 2008] presented a forecast of geomagnetic storm occurrence and its evaluation by using CME parameters such as location, speed, and earthward direction. They also presented, for the first time, a probability map that shows the occurrence fraction of geoeffective CMEs, in percentages, for given ranges of CME conditions. However, forecasting of geomagnetic storm strength based on CME parameters has not been widely investigated. Forecasting of geomagnetic storm strength could be more important than forecasting of geomagnetic storm occurrence, from a practical aspect. Regarding this, we develop an empirical model to predict geomagnetic storm strength by using only CME parameters and present an evaluation of the forecast capability of the model in this study.

[7] We present the data and discuss the geoeffectiveness of the CME parameters in section 2. We suggest a set of empirical formulae for the prediction of the strength of geomagnetic storms in section 3 and test the formulae in section 4. A brief summary and discussion are given in section 5.

## 2. Data and CME Geoeffectiveness

### 2.1. Data

[8] We used the CME events observed with the LASCO on board the Solar and Heliospheric Observatory (SOHO) [*Brueckner et al.*, 1995] during the period from 1997 to 2004. Their properties are compiled in the CME online catalogue (available at http://cdaw.gsfc.nasa.gov/CME_list/index.htm) [*Yashiro et al.*, 2004], and we used the measured CME speeds, angular widths, and position angles for each event found in the catalogue.

[9] Since our goal is to examine the CME-*Dst* relationship, including CME source parameters, we need to examine the frontside CMEs with well-identified source regions on the Sun. About 900 halo CMEs were detected during this period, and presumably half of them would have originated from the frontside. However, we could not use all of them, because it is hard to identify the associated *Dst* for either multiple events or weak events. We thus selected only strong and well-isolated CME events with clearly identified source regions on the Sun. Under this criterion, we end up with only 66 halo events associated with M-class and X-class flares for which we could confirm the matching *Dst*.

[10] To determine the CME location, we carefully compared the SOHO–LASCO images with the SOHO–EIT (Extreme ultraviolet Imaging Telescope) [*Delaboudiniere et al.*, 1995] running difference images. By investigating spatial and temporal closeness between the CME position and EUV features, such as brightening or flare-associated ejecting loops, we measured the source location of the CME. We also compared this with the flare lists of the Solar Flare Telescope (SOFT) [*Park et al.*, 1997; *Moon et al.*, 2000] published by the Korea Astronomy and Space Science Institute (KASI; available at http://sos.kasi.re.kr/korean/intranet/diary/flare.php) as well as by the National Geophysical Data Center (NGDC; available at ftp://ftp.ngdc.noaa.gov/STP/SOLAR_DATA/).

[11] Even if we know the source location of a CME, we cannot assume the propagation direction since all CMEs do not eject radially from the source region. In this respect, the direction parameter could be used to trace the CME's propagating direction at least near the Sun [*Moon et al.*, 2005]. If a CME is directly propagating toward the Earth, the shape of the CME front edge should be nearly symmetric, and the CME may trigger a geomagnetic storm. Otherwise, the shape should be quite asymmetric and the CME may not drive a geomagnetic storm. We therefore utilize the direction parameter as measured from the coronagraph observation for each event.

[12] We used magnetic field orientation data for the solar surface from *Song et al.* [2006]. They determined the magnetic field orientation angle $\theta$ by measuring the angle between the projection of the overlying potential field line

**Table 1.** Forecast Contingency Table

| | Observation | | |
|---|---|---|---|
| Prediction | Yes | No | Total |
| Yes | a (hits) | b (false alarms) | a + b |
| No | c (misses) | d (correct nulls) | c + d |
| Total | a + c | b + d | a + b + c + d |

determined by using a potential field model [*Abramenko*, 1986] on the solar surface and the direction toward the south pole by using SOHO–Michelson Doppler Imager (MDI) images (see Figure 3 of *Song et al.* [2006]).

[13] To identify geoeffective CMEs, we made CME-*Dst* pairs by adopting an empirical CME propagation model [*Gopalswamy et al.*, 2001] that estimates the arrival time of a CME at the Earth. Then, we determined the *Dst* minimum for a given CME by searching for the lowest value of hourly equatorial *Dst* values from the World Data Center for Geomagnetism in Kyoto (available at http://swdcwww.kugi.kyoto-u.ac.jp/) within a ±24 hour time window from the predicted CME arrival time. If a CME is predicted to arrive at the Earth and there is a *Dst* minimum within the time window, we selected this value as the result of the CME without any ambiguity. Most of our identifications are consistent with other studies [*Cane and Richardson*, 2003; *Zhang et al.*, 2007].

[14] According to *Gonzalez et al.* [1994], geomagnetic storms are classified as: (1) Intense storms, minimum *Dst* of −100 nT or less; (2) moderate storms, minimum *Dst* falls between −50 and −100 nT; and (3) weak or minor storms, minimum *Dst* falls between −30 and −50 nT. In particular, we call a event a super storm when its minimum *Dst* is −200 nT or less. In this study, we defined geomagnetic storms as geoeffective when *Dst* minimum is below −50 nT, so that 40 CMEs were found to be geoeffective among 66 events, and the mean probability of CME geoeffectiveness is about 61%, derived by considering frontside halo or partial halo CMEs associated with M-class and X-class flares.

[15] For statistical evaluation of the model, we adopted a contingency table that has been widely used in the meteorological forecasting literature [*Detman and Joselyn*, 1999]. Table 1 is a general form of the contingency table. In this table, "a" is the number of hits that were "yes" predicted and "yes" observed while "b" is the number of false alarms, that is, "yes" predicted but "no" observed. The misses, "c," represent "no" predicted but "yes" observed, and the correct nulls, "d," are "no" predicted and "no" observed. The statistics may then be computed from the contingency table. Thus, the probability of detection yes (PODy) is the proportion of "yes" observations that were correctly forecast, as estimated by a/(a + c). The probability of detection no (PODn) is the proportion of "no" observations that were correctly forecast, and is estimated by d/(b + d). The false alarm ratio (FAR) is the proportion of "yes" predictions that were incorrect, and is estimated by b/(a + b). The bias is the ratio of "yes" predictions to "yes" observations, and is estimated by (a + b)/(a + c). Finally, the critical success index (CSI) is the successful rate and is defined as the proportion of hits that were either predicted or observed, as estimated by a/(a + b + c) [*Smith et al.*, 2000]. Good forecasts are indicated by statistical values that are close to 1, except for FAR, which should be close to 0 for a good forecast.

### 2.2. Geoeffectiveness of CME Parameters

[16] To gain an idea for a storm prediction model based on CME parameters, we examined the relationships between the storm strength (*Dst* minimum) and each of the following parameters: CME source location, speed, earthward direction, and magnetic field orientation (generally in the active or flare location) at its source region.

[17] To examine the geoeffectiveness of location parameter, initially, we investigated two parameters as proxies of the CME source location: longitude and the cosine angle between the Sun–Earth line and the radial axis of a CME source region. Here the cosine angle includes both the effects of latitude and longitude. While the source locations of the geoeffective CMEs are systematically distributed in longitude, most CMEs including nongeoeffective CMEs are located within ±40° in latitude. In addition, we did not find a systematic dependence of geoeffective CMEs on latitude so that we considered only the longitude as the location parameter. Figure 1 shows the longitudinal distribution of CME. As shown in Figure 1, the longitude of geoeffective CMEs is asymmetrical with the majority located on the west side of the central meridian. This result is consistent with those in other studies [*Wang et al.*, 2002; *Kim et al.*, 2005].

[18] To reflect the asymmetric pattern of the longitudinal distribution on the storm prediction model, we found an offset value which represents an axis to produce the symmetrical distribution of CME longitudes as follows. We compared the linear Pearson correlation coefficients (cc) between *Dst* index and the distance from the offset and also compared the critical success indices (CSIs), which indicate the success rates of geomagnetic storm forecast by using an offset value. As shown in Table 2, the best offset value is 15°W when considering both correlation coefficient and the storm forecast capability (i.e., CSI). That is, even though the 20°W offset has a better correlation coefficient (0.26) than W15° it has a lower CSI. Figure 2 shows the relationship between *Dst* index and the distance from the offset for 66 events.

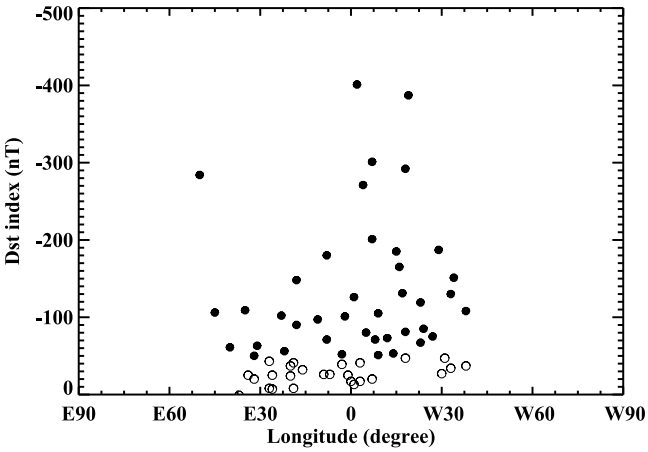


**Figure 1.** The longitudinal distribution for 66 events. The *x* axis is longitude and the *y* axis is *Dst* index. The closed circles represent the geoeffective CME and the empty circles represent nongeoeffective CMEs.

**Table 2.** The Linear Pearson Correlation Coefficient Between *Dst* Index and the Distance From the Offset and the Critical Success Index of Our Geomagnetic Storm Forecast Method for Several Given Offset Values

| Offset | cc[a] | CSI[b] |
|---|---|---|
| 0°W | 0.06 | 0.52 |
| 5°W | 0.17 | 0.57 |
| 10°W | 0.22 | 0.54 |
| 15°W | 0.25 | 0.56 |
| 20°W | 0.26 | 0.54 |
| 25°W | 0.23 | 0.52 |
| 30°W | 0.21 | 0.50 |

[a]Correlation coefficient.
[b]Critical success index.

[19] We examined the relationship between *Dst* index and CME speed as shown in Figure 3. We used the linear plane-of-sky speed obtained by fitting a straight line to the height-time measurements from the SOHO–LASCO CME online catalog. The linear speed indicates an average speed within the LASCO field of view. *Srivastava and Venkatakrishnan* [2004] showed that for intense storm events ($Dst \leq -100$ nT), the plane-of-sky speeds of halo CMEs are correlated with the strength of geomagnetic storms (cc = −0.66). But as shown in Figure 3, even slow halo CMEs can trigger geomagnetic storms.

[20] As an important parameter for geomagnetic storm forecast, we considered the empirically-determined earthward direction parameter following *Moon et al.* [2005] and *Kim et al.* [2008]. It offers many advantages to forecasting of geomagnetic storms since it can be determined directly from coronagraph observations and is applicable to most of the halo CMEs, even though the CME locations are not known. And it includes both the CME propagation and angular width effect [*Moon et al.*, 2009]. Conceptually, the CME source location and the direction parameter should be consistent with each other if all CMEs are radially ejected. However, we found a low correlation (cc = 0.17) between CME source longitude and the direction parameter, as shown in Figure 4. Based on this result, we regarded the two parameters as independent in our model. We speculate from the low correlation that the direction of CME propagation is strongly affected by its ambient magnetic field structures.

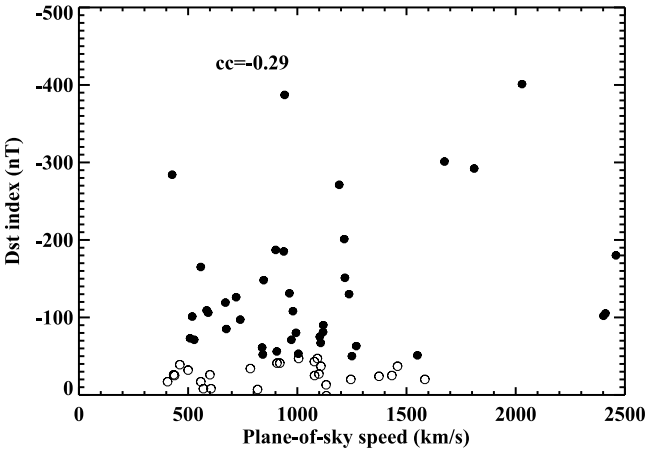


**Figure 3.** The relationship between *Dst* index and plane-of-sky speed for 66 events.

[21] Thus we examined the relationship between *Dst* index and earthward direction parameter. In Figure 5, we plotted the *Dst* index versus the earthward direction parameter for 66 events. As shown in the figure, the direction parameter has a relatively high correlation coefficient with geomagnetic storm strength (cc = −0.60), and is higher than that with other parameters.

[22] Magnetic reconnections between southward IMF and the northwardly directed geomagnetic field occur at the dayside magnetopause and then transport energy from the solar wind into the magnetosphere [*Dungey*, 1963; *Gonzalez et al.*, 1999].Thus the magnetic field orientation within a CME source region is an important factor that should be considered for geomagnetic storm forecasts. If we assume that the magnetic field orientation of a CME is preserved during its interplanetary transit to Earth, we can expect that a CME with a southward magnetic field orientation in its source region will be more geoeffective, thereby causing a geomagnetic storm. Based on this idea, we examined the magnetic field orientation angle $\theta$ of the CME source region

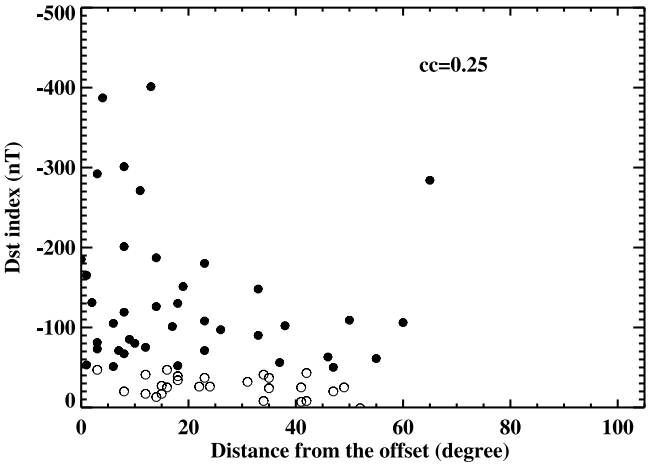


**Figure 2.** The relationship between *Dst* index and distance from the offset for 66 events.

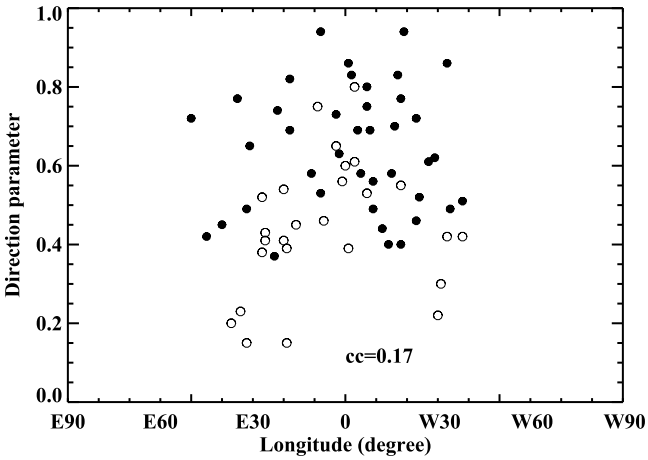


**Figure 4.** The relationship between CME longitude and direction parameter for 66 events.

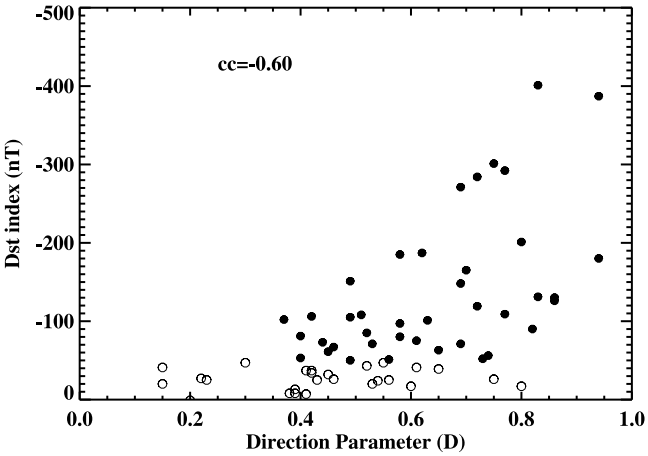


**Figure 5.** The relationship between *Dst* index and the earthward direction parameter for 66 events.

for 66 events. Figure 6 shows a very low correlation (cc = 0.12) between *Dst* index and magnetic field orientation, but all CME source regions associated with the super storms ($Dst \leq -200$ nT) have southward field orientations and are located on the left side of the vertical dashed line that indicates 90°. Several CMEs that have northward magnetic field orientations also caused intense geomagnetic storms ($Dst \leq -100$ nT).

[23] To compare the geoeffectiveness and to adopt all parameters into geomagnetic storm prediction formulae, we made all parameters between 0 to 1. The parameterized longitude ($L$) is defined as the distance from the offset divided by the maximum value. Since the maximum CME speed is just below 2500 km $s^{-1}$ for all halo CMEs that occurred from 1997 to 2003, we used the parameterized speed ($V$), which is defined as the speed divided by the maximum CME speed. Even if a CME is faster than 2500 km $s^{-1}$, our model works properly. We also defined magnetic field orientation ($M$) by dividing the magnetic field orientation angle by 180°. A CME is southward when $M$ is less than 0.5, otherwise, the CME is northward (i.e., $M > 0.5$). Direction parameter ($D$) is already parameterized because this value is the ratio of the shortest to the longest distance of the CME front as measured from the solar center. All parameters are unitless.

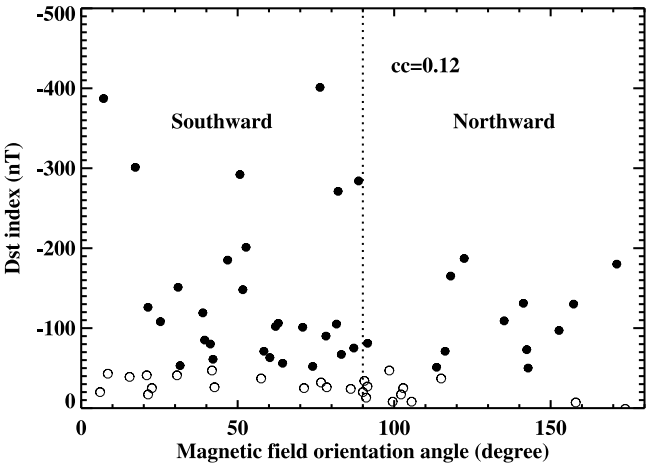


**Figure 6.** The relationship between *Dst* index and the magnetic field orientation for 66 events. The vertical dotted line represents a magnetic field orientation angle $\theta$ of 90°.

[24] Table 3 lists the correlation coefficients with *Dst* index for each CME parameter. As shown in Table 3, we can easily see that the earthward direction is the best parameter to select geoeffective CMEs and much better than the other parameters (cc = −0.60). The magnetic field orientation has an even lower correlation coefficient (cc = 0.12) than those for location and speed parameters.

## 3. Storm Prediction Model

[25] Although the above comparisons suggest general dependencies of geomagnetic storm strength on CME parameters, no single CME parameter is found to significantly correlate with geomagnetic storm strength. This implies that a geomagnetic storm cannot be predicted by any single CME parameter, but depends on all of these parameters in a more complicated way. We thus propose a model in which the geomagnetic storm strength (*Dst* in nT) depends on four major parameters in the form [*Press et al.*, 2007]:

$$Dst = \text{constant} + \alpha L + \beta V + \gamma D + \delta M, \quad (1)$$

where $L$ is normalized CME source location, $V$ is normalized CME speed, $D$ is the earthward direction parameter, and $M$ is normalized magnetic field orientation angle. $\alpha$, $\beta$, $\gamma$, and $\delta$ are constant coefficients that we will determine on an empirical basis. Here a linear relationship between *Dst* and the four CME parameters is assumed as a simple possibility, although a more complicated dependence may be sought.

[26] Meanwhile, in Figure 6 we find that southward oriented CMEs produced super storms while northward CMEs produced none. These six super storms are evenly located in a southward orientation area. We speculate that the magnetic field orientation sign of a CME source region is more important for CME geoeffectiveness than the magnetic field orientation angle itself. Based on the above idea, we divided all CMEs into two classes according to their magnetic field orientation signs and applied a multiple linear regression method using three independent variables ($L$, $V$, and $D$). In addition, we excluded the longitude parameter for southward events, since its partial-correlation coefficient (P-cc) with *Dst* index is very low as shown in Table 4. Table 4 shows the partial-correlation coefficients of each parameter. For the southward events, the earthward direction has the best partial correlation coefficient (−0.59), which means it is the most significant parameter, however, speed is

**Table 3.** Correlation Coefficients Between Geoeffective Parameters and *Dst* Index

| Parameter | cc |
|---|---|
| Location | 0.25 |
| Speed | −0.29 |
| Direction | −0.60 |
| Magnetic field orientation | 0.12 |

**Table 4.** Partial Correlation Coefficients of Each Parameter

| | $L^a$ | $V^b$ | $D^c$ |
|---|---|---|---|
| South | 0.001 | −0.45 | −0.59 |
| North | 0.22 | −0.23 | −0.74 |

[a]Location.
[b]Speed.
[c]Direction.

also somewhat effective (P-cc = −0.45) but the P-cc for location is negligible (0.001). Thus, we made the formula by using just two parameters for southward events. In the case of northward events, the earthward direction parameter (P-cc = −0.74) was more important than the P-cc values for the other two parameters.

[27] Finally, the storm prediction formulae for halo CMEs are given by

$$Dst = 172 - 199 \times V - 337 \times D, \quad (2)$$

for southward events, and

$$Dst = 47 + 53 \times L - 47 \times V - 202 \times D, \quad (3)$$

for northward events. Here the CME parameters, $L$, $V$, and $D$ are all normalized to their maxima so that their values always lie between 0 and 1.

[28] We examined the relationship between the observed *Dst* index and the predicted *Dst* index calculated using these formulae. Figure 7 shows the relationship between observed and predicted *Dst* indices for 42 southward events, while Figure 8 shows the same relationship for 24 northward events. As shown in Figures 7 and 8, the relationship between observed *Dst* index and the predicted *Dst* index for northward events (cc = 0.80) is better than that for southward events (cc = 0.66). The lower correlation found for the southward events is partly due to the presence of super storms ($Dst \leq -200$ nT). This may imply that there are other factors for super storms which do not well correlate with the CME parameters. To improve our model, we need to take into account such factors, which we will discuss in section 5. Note, however, that we can, at least, predict the occurrence of super storms based on the above formulae, although we cannot accurately predict the *Dst* values of the super storms.

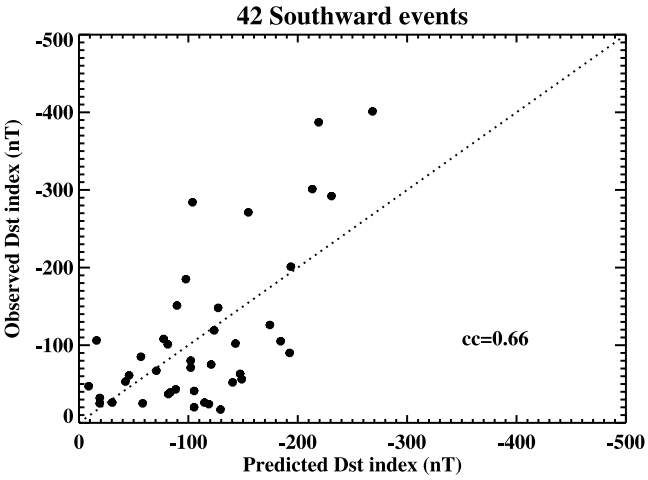


**Figure 7.** The relationship between observed *Dst* index and predicted *Dst* index for 42 southward events.

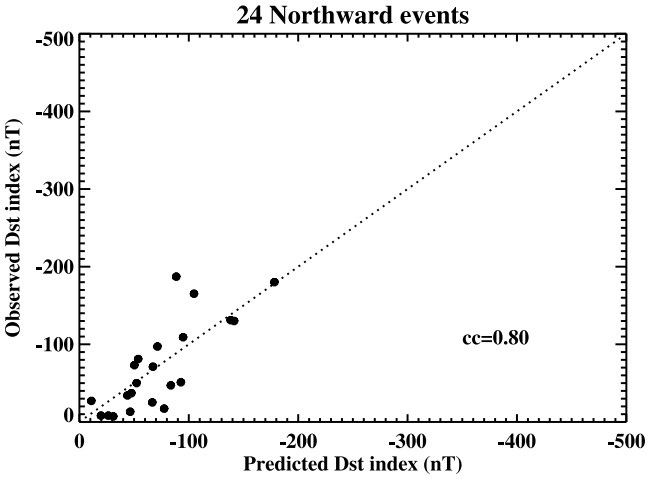


**Figure 8.** The relationship between observed *Dst* index and predicted *Dst* index for 24 northward events.

## 4. Test of the Model

[29] As a verification of the model, we applied the storm prediction model to an independent set of CMEs. The test sample consists of 31 halo CMEs observed from 2004 to 2006 which were selected from the CME catalog by *Smith et al.* [2009]. We selected only isolated and fast ($v \geq 1000$ km s$^{-1}$) events from the catalog, because it is ambiguous to set a CME–*Dst* relationship in the case of multiple CME events. The model *Dst* index is calculated using equations (2) and (3) and is compared with the observed *Dst* index (Figure 9). The resulting correlation is rather poor (cc = 0.44). We expected this model to be able to better predict the *Dst* index, but in fact the model is not yet particularly good at it. However, our model does appear to be quite good at predicting the occurrence of a geoeffective event. If the *Dst* index calculated by the model is less than

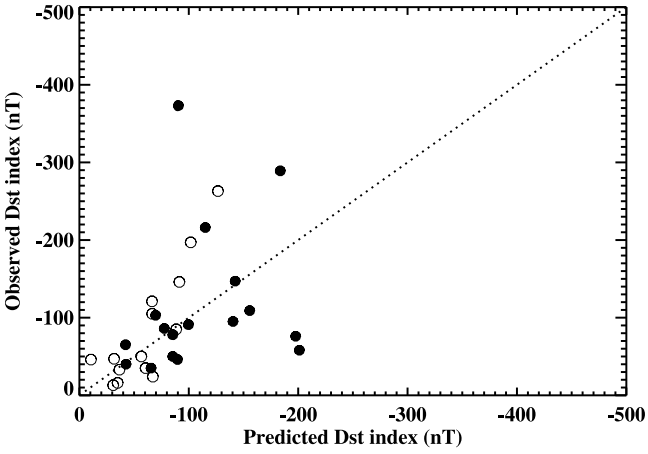


**Figure 9.** The relationship between observed *Dst* index and predicted *Dst* index for 31 events from 2004 to 2006. Filled circles represent southward events and empty circles represent northward events.

**Table 5.** Contingency Table Based on the Storm Prediction Formulae

| | Observation | | |
|---|---|---|---|
| Prediction | Yes | No | Total |
| Yes | 20 | 4 | 24 |
| No | 1 | 6 | 7 |
| Total | 21 | 10 | 31 |

−50 nT, we can predict a geomagnetic storm occurrence. In Figure 9, there are 21 storms with actual *Dst* below −50 nT. Among them, 20 storms have been predicted by our model to have *Dst* values below −50 nT.

[30] Table 5 shows the 2 × 2 contingency table between predictions and observations, where 24 of 31 CMEs are classified as yes predictions and 21 CMEs are found to be yes observations. Each value in this contingency table represents the success or failure of this forecasting experience, and includes hits (20), false alarms (4), misses (1), and correct nulls (6). Following the method we described in section 2.1, we determined the statistics of the forecast evaluation (Table 6). The PODy is 0.95, which means if there is a geomagnetic storm, we can correctly forecast with the probability of 95%, while the PODn is 0.60. The FAR and the bias are 0.17 and 1.14, respectively. The CSI, used as an important index for evaluation of the forecast, is 0.80.

## 5. Summary and Discussion

[31] In this work, we have developed an empirical storm forecast model based on CME parameters. It is very meaningful in that it can give us about 2–3 days of advance notice to prepare for geomagnetic storms. Other studies, still in very early stages [*Dryer*, 1998], use physics-based models that employ observations of flares or CME occurrences and coronal shock-induced metric radio frequency drifts [*Cho et al.*, 2003; *Fry et al.*, 2003; *Odstrcil*, 2003; *Dryer et al.*, 2004; *McKenna-Lawlor et al.*, 2006] to predict CME or their shocks' arrivals at Earth. These studies use such observations (such as CME cone shapes and ad hoc overpressure or momentum pulses) to mimic the basically unknown physical processes in the originating form of solar activity. In an operational context, space weather forecasters often prefer empirical approaches pending more extensive real time verification of the physics-based models.

[32] Our empirical model is solely based on CME parameters, including longitude, speed, direction parameter, and magnetic field orientation of an overlaying potential field at the CME source region. We examined the relationship, in our empirical approach, between *Dst* index and each parameter for 66 frontside halo CMEs in detail. The following results were considered to provide storm prediction formulae.

[33] 1. Since the source locations of geoeffective CMEs are asymmetrical in longitude, we adopt an offset. A 15°W offset from the central meridian gives the best correlation between source location and storm strength.

[34] 2. The direction parameter has the best correlation with storm strength.

[35] 3. Consideration of two groups of CMEs according to their magnetic field orientation (southward or northward) provides a better forecast. Thus, we divide CMEs into two groups according to their magnetic field orientation.

[36] As a result, we suggest two empirical formulae, *Dst* (in nT) = 172–199 × $V$ − 337 × $D$ and *Dst* (in nT) = 47 + 53 × $L$ − 47 × $V$ − 202 × $D$, for southward and northward magnetic field orientations, respectively. For the southward events, we found that the earthward direction is the most effective parameter, while speed is also somewhat effective, but the location effect is negligible. In the case of northward events, we found that the earthward direction parameter is more dominant than other parameters. The relationship between observed *Dst* index and predicted *Dst* index for northward events is better than that for southward events.

[37] When we evaluate the forecast based on these formulae by comparing predicted and observed storm occurrence from 2004 to 2006, the PODy, PODn, FAR, and CSI are 0.95, 0.60, 0.17, and 0.80, respectively. The correlation coefficient of the relation between predicted and observed storm strengths is 0.44. This result shows that a forecast based on the storm prediction model is improved in comparison with a forecast based on criteria of the CME parameters (PODy = 0.86, PODn = 0.61, FAR = 0.42, and CSI = 0.53; *Kim et al.*, 2008).

[38] This work shows a sufficient possibility of geomagnetic storm prediction for real time forecasting using only initially observed CME parameters, which will allow us to make an earlier warning of specific *Dst* minimum levels of geomagnetic storms 2–3 days in advance. To make such a realtime forecast of a geomagnetic storm, we first have to check whether the magnetic field orientation of a frontside halo CME is southward or northward by using the SOHO–MDI magnetogram. Then we can choose an appropriate formula depending on the magnetic field orientation. As the second step, we have to determine the values of parameters, $L$, $V$, and $D$, which are parameterized to be between 0 to 1. If the calculated *Dst* is less than −50 nT, we can forecast a geomagnetic storm occurrence as well as its strength.

[39] Our results indicate that the prediction of geomagnetic storm strength based on the formulae is reliable and useful for space weather forecast. However, there are some errors and the formula tends to underestimate the *Dst* index in strong southward events. To improve the model, we have to consider interplanetary (IP) shocks as well as real-time solar and near Earth conditions for more accurate physics-based forecasts [*Dryer*, 1998]. It is also well known that the geomagnetic storm strength strongly relates with southward magnetic field in the solar wind [*Burton et al.*, 1975; *Tsurutani et al.*, 1998; *Tsurutani*, 2001 and references therein; *Kane*, 2008]. One may expect that the orientation of the overlying field in the CME source region, $M$, among

**Table 6.** Statistical Parameters for the Forecast Evaluation Using the Storm Prediction Formulae

| Statistics | Value |
|---|---|
| Probability of detection | |
| Yes (PODy) | 0.95 |
| No (PODn) | 0.60 |
| False alarm ratio (FAR) | 0.17 |
| Bias | 1.14 |
| Critical success index (CSI) | 0.80 |

other parameters, would be the most relevant to that of the IMF. We, however, found no good correlation between *M* and the observed *Dst*. This low correlation may imply that the magnitude and orientation of the IMF near the Earth are not simply related to those of the fields in the CME source region. One reason could be that CME magnetic fields may rotate during passage from the Sun to the Earth and obscures the importance of magnetic field orientation as a factor in the storm prediction. A more detailed investigation of the evolution of CME magnetic fields during passage is needed to understand this issue.

[40] **Acknowledgments.** This work was supported by the Korea Research Foundation grant funded by the Korean Government (MOEHRD) (KRF-2006-612-C00014, KRF-2005-202-C00158) and by the "Development of Korean Space Weather Center," the project of KASI, and the KASI basic research fund. Y.J.M. has been supported by the WCU grant (R31-10016) funded by the Korean Ministry of Education, Science and Technology and by the Korea Research Foundation grant funded by the Korean Government (MOEHRD, Basic Research Promotion Fund) (KRF-2008-314-C00158, 20090071744). M.D. was supported by NASA's Living With a Star progrram via grant NAG5-12527 to Exploration Physics International, Inc. M.D. also thanks NOAA's Space Weather Prediction Center for their hospitality during his emeritus status. J.L. was supported NSF grants AST-0908344 and ANT-083995 and NASA grant NAS5-01072. H.W. was supported by NASA grant NNX08-8AQ90G and NSF grant ATM-0839216. The CME catalog used here is generated and maintained by NASA and the Catholic University of America in cooperation with the Naval Research Laboratory. The *Dst* index is provided by the World Data Center for Geomagnetism at Kyoto University.

[41] Philippa Browning thanks the reviewers for their assistance in evaluating this manuscript.

## References

Abramenko, V. I. (1986), The accuracy of potential field restoration using the Neumann problem, *Solnechnye Dann. Bull. Akad. Nauk SSSR*, *1986*, 83–89.

Brueckner, G. E., et al. (1995), The large angle spectroscopic coronagraph (LASCO), *Sol. Phys.*, *162*, 357–402, doi:10.1007/BF00733434.

Brueckner, G. E., et al. (1998), Geomagnetic storms caused by coronal mass ejections (CMEs): March 1996 through June 1997, *Geophys. Res. Lett.*, *25*, 3019—3022, doi:10.1029/98GL00704.

Burton, R. P., R. L. McPherron, and C. T. Russell (1975), An empirical relationship between interplanetary conditions and *Dst*, *J. Geophys. Res.*, *80*, 4204–4214, doi:10.1029/JA080i031p04204.

Cane, H. V., and I. G. Richardson (2003), Interplanetary coronal mass ejections in the near-Earth solar wind during 1996–2002, *J. Geophys. Res.*, *108*(A4), 1156, doi:10.1029/2002JA009817.

Cho, K.-S., Y.-J. Moon, M. Dryer, C. D. Fry, Y.-D. Park, and K.-S. Kim (2003), A statistical comparison of interplanetary shock and CME propagation models, *J. Geophys. Res.*, *108*(A12), 1445, doi:10.1029/2003JA010029.

Delaboudiniere, J. P., et al. (1995), EIT: Extreme-Ultraviolet Imaging Telescope for the SOHO Mission, *Sol. Phys.*, *162*, 291–312, doi:10.1007/BF00733432.

Detman, T., and J. Joselyn (1999), Real-time *Kp* predictions from ACE real time solar wind, *AIP Conf. Proc.*, *471*, 729–732, doi:10.1063/1.58720.

Dryer, M. (1998), Multidimensional, magnetohydrodynamic simulation of solar-generated disturbances: Space weather forecasting of geomagnetic storms, *AIAA J.*, *36*(3), 365–370, doi:10.2514/2.405.

Dryer, M., Z. Smith, C. D. Fry, W. Sun, C. S. Deehr, and S.-I. Akasofu (2004), Real-time shock arrival predictions during the "Halloween 2003 epoch", *Space Weather*, *2*, S09001, doi:10.1029/2004SW000087.

Dungey, J. W. (1963), Interactions of solar plasma with the geomagnetic field, *Planet. Space Sci.*, *10*, 233–237.

Fry, C. D., M. Dryer, Z. Smith, W. Sun, C. S. Deehr, and S.-I. Akasofu (2003), Forecasting solar wind structures and shock arrival times using an ensemble of models, *J. Geophys. Res.*, *108*(A2), 1070, doi:10.1029/2002JA009474.

Gonzalez, W. D., J. A. Joselyn, Y. Kamide, H. W. Kroehl, G. Rostoker, B. T. Tsurutani, and V. M. Vasyliunas (1994), What is a geomagnetic storm?, *J. Geophys. Res.*, *99*, 5771–5792.

Gonzalez, W. D., B. T. Tsurutani, and A. L. Clua de Gonzalez (1999), Interplanetary origin of geomagnetic storms, *Space Sci. Rev.*, *88*, 529–562, doi:10.1023/A:1005160129098.

Gopalswamy, N., A. Lara, R. P. Lepping, M. L. Kaiser, D. Berdichevsky, and O. C. St. Cyr (2000), Interplanetary acceleration of coronal mass ejections, *Geophys. Res. Lett.*, *27*, 145–148, doi:10.1029/1999GL003639.

Gopalswamy, N., A. Lara, S. Yashiro, M. L. Kaiser, and R. A. Howard (2001), Predicting the 1-AU arrival times of coronal mass ejections, *J. Geophys. Res.*, *106*, 29,207–29,217, doi:10.1029/2001JA000177.

Gopalswamy, N., S. Yashiro, and S. Akiyama (2007), Geoeffectiveness of halo coronal mass ejections, *J. Geophys. Res.*, *112*, A06112, doi:10.1029/2006JA012149.

Kane, R. P. (2008), Limitations of the utility of CMEs for forecasting timings and magnitudes of geomagnetic *Dst* storms, *Indian J. Radio Space Phys.*, *37*, 303–311.

Kang, S.-M., Y.-J. Moon, K.-S. Cho, Y.-H. Kim, Y. D. Park, J.-H. Baek, and H.-Y. Chang (2006), Coronal mass ejection geoeffectiveness depending on field orientation and interplanetary coronal mass ejection classification, *J. Geophys. Res.*, *111*, A05102, doi:10.1029/2005JA011445.

Kim, K.-H., Y.-J. Moon, and K.-S. Cho (2007), Prediction of the 1-AU arrival times of CME-associated interplanetary shocks: Evaluation of an empirical interplanetary shock propagation model, *J. Geophys. Res.*, *112*, A05104, doi:10.1029/2006JA011904.

Kim, R.-S., K.-S. Cho, Y.-J. Moon, Y.-H. Kim, Y. Yi, M. Dryer, S.-C. Bong, and Y.-D. Park (2005), Forecast evaluation of the coronal mass ejection (CME) geoeffectiveness using halo CMEs from 1997 to 2003, *J. Geophys. Res.*, *110*, A11104, doi:10.1029/2005JA011218.

Kim, R.-S., K.-S. Cho, Y.-J. Moon, M. Dryer, Y. Yi, J. Lee, K.-H. Kim, H. Wang, H. Song, and Y.-D. Park (2008), CME earthward direction as an important geoeffectiveness indicator, *Astrophys. J.*, *677*, 1378–1384.

McKenna-Lawlor, S. M. P., M. Dryer, M. D. Kartalev, Z. Smith, C. D. Fry, W. Sun, C. S. Deehr, K. Kecskemety, and K. Kudela (2006), Near real-time predictions of the arrival at Earth of flare-related shocks during Solar Cycle 23, *J. Geophys. Res.*, *111*, A11103, doi:10.1029/2005JA011162.

Moon, Y.-J., Y. D. Park, H. C. Seong, C. W. Lee, K. J. Sim, and H. S. Yun (2000), A near real-time flare alerting system based on GOES soft X-ray flux, *J. Korean Astron. Soc.*, *33*, 123–126.

Moon, Y.-J., K.-S. Cho, M. Dryer, Y.-H. Kim, S.-C. Bong, J. Chae, and Y. D. Park (2005), New geoeffective parameters of very fast halo coronal mass ejections, *Astrophys. J.*, *624*, 414–419, doi:10.1086/428880.

Moon, Y.-J., R.-S. Kim, and K.-S. Cho (2009), Geometrical implication of the CME earthward direction parameter and its comparison with cone model parameters, *J. Korean Astron. Soc.*, *42*, 27–32.

Odstrcil, D. (2003), Modeling 3D solar wind structure, *Adv. Space Res.*, *32*, 497–506, doi:10.1016/S0273-1177(03)00332-6.

Park, Y. D., Y.-J. Moon, B. H. Jang, and K. J. Sim (1997), Observation system of solar flare telescope, *Publ. Korean Astron. Soc.*, *12*, 35–45.

Pevtsov, Alexei A., and Richard C. Canfield (2001), Solar magnetic fields and geomagnetic events, *J. Geophys. Res.*, *106*, 25,19–1–25,197, doi:10.1029/2000JA004018.

Press, W., S. A. Teukolsky, W. T. Vetterling, and B. P. Flannery (2007), *Numerical Recipes: The Art of Scientific Computing*, 3rd edition, Cambridge Univ. Press, Cambridge, U.K.

Smith, Z., M. Dryer, M. E. Ort, and W. Murtagh (2000), Performance of interplanetary shock prediction models: STOA and ISPM, *J. Atmos. Sol. Terr. Phys.*, *62*, 1265–1274, doi:10.1016/S1364-6826(00)00082-1.

Smith, Z. K., R. Steenburgh, C. D. Fry, and M. Dryer (2009), Predictions of interplanetary shock arrivals at Earth: Dependence of forecast outcome on the input parameters, *Space Weather*, *7*, S12005, doi:10.1029/2009SW000500.

Song, H., V. Yurchyshyn, G. Yang, C. Tan, W. Chen, and H. Wang (2006), The automatic predictability of super geomagnetic storms from halo CMEs associated with large solar flares, *Sol. Phys.*, *238*, 141–165, doi:10.1007/s11207-006-0164-8.

Srivastava, N. (2005), Predicting the occurrence of super-storms, *Ann. Geophys.*, *23*, 2989–2995.

Srivastava, N., and P. Venkatakrishnan (2004), Solar and interplanetary sources of major geomagnetic storms during 1996–2002, *J. Geophys. Res.*, *109*, A10103, doi:10.1029/2003JA010175.

Tsurutani, B. T. and W. D. Gonzales (Eds.) (1998), *From the Sun: Auroras, Magnetic Storms, Solar Flares, Cosmic Rays*, AGU, Washington, D. C.

Tsurutani, B. T. (2001), The interplanetary causes of magnetic storms, substorms, and geomagnetic quiet, in *Space Storms and Space Weather Hazards*, edited by I. A. Daglis, pp. 103–130, Kluwer Acad., Dordrecht, Netherlands.

Venkatakrishnan, P., and B. Ravindra (2003), Relationship between CME velocity and active region magnetic energy, *Geophys. Res. Lett.*, *30*(23), 2181, doi:10.1029/2003GL018100.

Wang, Y. M., P. Z. Ye, S. Wang, G. P. Zhau, and J. Wang (2002), A statistical study on the geoeffectiveness of Earth-directed coronal mass ejections from March 1997 to December 2000, *J. Geophys. Res.*, *107*(A11), 1340, doi:10.1029/2002JA009244.

Webb, D. F. (2002), CMEs and the solar cycle variation in their geoeffectiveness, *Proc. Sol. Heliospheric Obs. 11 Symp.*, *2002*, 409–419.

Yashiro, S., N. Gopalswamy, G. Michalek, O. C. St. Cyr, S. P. Plunkett, N. B. Rich, and R. A. Howard (2004), A catalog of white light coronal mass ejections observed by the SOHO spacecraft, *J. Geophys. Res.*, *109*, A07105, doi:10.1029/2003JA010282.

Zhang, J., et al. (2007), Solar and interplanetary sources of major geomagnetic storms ($Dst \leq -100$ nT) during 1996–2005, *J. Geophys. Res.*, *112*, A10102, doi:10.1029/2007JA012321.

K.-S. Cho, Solar and Space Weather Research Group, Korea Astronomy and Space Science Institute, Daejeon, KR-305-348, Korea.

M. Dryer, National Oceanic and Atmospheric Administration, Boulder, CO 80305, USA.

K.-H. Kim, School of Space Research, Kyung Hee University, Yongin, KR-446-701, Korea.

R.-S. Kim, Y. H. Kim, and Y. Yi, Department of Astronomy and Space Science, Chungnam National University, Daejeon, KR-305-754, Korea. (rskim@cnu.ac.kr)

J. Lee, Department of Physics, New Jersey Institute of Technology, Newark, NJ US-07102, USA.

Y.-J. Moon, School of Space Research, Kyung Hee University, Yongin, KR-446-701, Korea.

Y.-D. Park, Solar and Space Weather Research Group, Korea Astronomy and Space Science Institute, Daejeon, KR-305-348, Korea.

H. Wang, Department of Physics, New Jersey Institute of Technology, Newark, NJ US-07102, USA.